Polymer electrolytes containing guanidinium-based polymeric ionic liquids for rechargeable lithium batteries

Mingtao Li [a], Li Yang [a,b,*], Shaohua Fang [a,b], Siming Dong [a], Shin-ichi Hirano [b], Kazuhiro Tachibana [c]

[a] *School of Chemistry and Chemical Technology, Shanghai Jiaotong University, Shanghai 200240, China*
[b] *Hirano Institute for Materials Innovation, Shanghai Jiaotong University, Shanghai 200240, China*
[c] *Department of Chemistry and Chemical Engineering, Faculty of Engineering, Yamagata University, Yamagata 992-8510, Japan*

ABSTRACT

The electrochemical properties of solvent-free, quaternary polymer electrolytes based on a novel polymeric ionic liquid (PIL) as polymer host and incorporating 1g13TFSI ionic liquid, LiTFSI salt and nano-scale silica are reported. The PIL–LiTFSI–1g13TFSI–SiO$_2$ electrolyte membranes are found to be chemically stable even at 80 °C in contact with lithium anode and thermally stable up to 320 °C. Particularly, the quaternary polymer electrolytes exhibit high lithium ion conductivity at high temperature, wide electrochemical stability window, time-stable interfacial resistance values and good lithium stripping/plating performance. Batteries assembled with the quaternary polymer electrolyte at 80 °C are capable to deliver 140 mAh g^{-1} at 0.1C rates with very good capacity retention.

1. Introduction

Rechargeable lithium metal polymer batteries (LMPBs) are considered to be the most probable next generation of power sources for portable electronic devices and electronic vehicles because of their high energy density and flexible characteristics [1]. However, the performance of LMPBs is still limited by low ionic conductivities of solid polymer electrolytes (SPEs) and bad interfacial properties between SPEs and electrodes. Thus, many different approaches have been pursued to enhance the ionic conductivity of the Li$^+$-cation-conducting SPEs and their interfacial properties [2–4].

Recently, the incorporation of non-volatile, non-flammable ionic liquids (ILs) into polymer electrolytes has been a very promising approach to improve the ionic conductivity and the interfacial property [5–11]. Most of the research work focused on ILs based upon imidazolium and pyrrolidinium cations and bis(trifluoromethanesulfonyl)imide anions. The imidazolium ILs have been widely studied because of their low viscosity, high ionic conductivity, and high anodic stability [7,12–14]. The pyrrolidinium ILs have been found to have a high cathodic stability and relatively high ionic conductivity [6,8,11,15–17]. A nanocomposite polymer electrolyte incorporating an IL [*n*-

butyl-3-methylimidazolium bis(trifluoromethanesulfonyl)imide (BMITFSI)] and poly(vinylidene fluoride-*co*-hexafluoropropylene) [PVdF-HFP] has been reported [13]. The addition of BMITFSI in polymer electrolytes results in high ionic conductivity at room temperature. The cells with BMITFSI show good interfacial stability and oxidation stability over 5.5 V. With respect to unsaturated cyclic and non-cyclic ammonium quaternary cations, pyrrolidinium cations show a much wider cathodic decomposition potential. The cycle behavior and rate performance of solid-state Li/LiFePO$_4$ polymer electrolyte batteries incorporating the *N*-methyl-*N*-propylpyrrolidinium bis(trifluoromethanesulfonyl)imide (PYR$_{13}$TFSI) room temperature IL into the P(EO)$_{20}$ LiTFSI electrolyte and the cathode have been investigated at 40 °C [10]. The battery shows excellent reversible cycling stability with a capacity fade lower than 0.06% per cycle over about 500 cycles at various current densities. To our knowledge, the hosts of polymer electrolytes incorporating IL are mostly focused on the traditional polymer such as PEO and PVdF-HFP.

Polymeric ionic liquids (PILs) to be used as hosts for polymer electrolytes have been attracting much attention because of their high ionic conductivity and chemical compatibility toward ILs [18–20]. In general, PILs are obtained through polymerization of ionic liquid monomers. In comparison with other polymers, PILs used as hosts in ionic liquids based polymer electrolytes exhibit unique features. PILs and corresponding ILs have good chemical affinity. A completely compatible combination between PILs and ILs makes the polymer electrolytes rather stable, which minimizes phase separation and leakage phenomena. When the PILs

* Corresponding author at: School of Chemistry and Chemical Technology, Shanghai Jiaotong University, Shanghai 200240, China. Tel.: +86 21 54748917; fax: +86 21 54741297.
  E-mail address: liyangce@sjtu.edu.cn (L. Yang).

were used in the electronic devices, the significant enhancement in cycling stability and durability has been observed [18].

In a previous work, a series of PILs based on guanidinium cations combining different anions, such as BF_4^-, PF_6^-, ClO_4^- and $N(CF_3SO_2)_2^-$, have been synthesized by our group [21], and their thermal properties, electrochemical stabilities and ionic conductivity were characterized. With the aim of developing highly conductively polymer electrolytes, we continue to synthesize new PILs. Herein, we present another guanidinium-based PIL with TFSI$^-$ anions, which was synthesized by copolymerization of a guanidinium ionic liquid monomer with methyl acrylate. Comparing with the reported PILs, the new PIL has a longer alkyl chain in the structure of guanidinium cations, which increases the rigid of the PIL chains, and results in sufficient mechanical strength and good ionic liquid retention for the PIL membrane [22,23]. In addition, to the applications of lithium batteries, a quaternary polymer electrolyte based on the PIL as polymer host in combination with a guanidinium ionic liquid, LiTFSI salt and nano-size SiO_2 were prepared. Various quaternary electrolytes having different weight compositions were physicochemical characterized. The performance of LMPBs with the quaternary electrolytes was measured at 80 °C.

2. Experimental

2.1. Reagents and materials

2,2′-azobisisobutyronitrile (AIBN) methyl acrylate and allyl bromide (98%) were purchased from Alfa Aesar. Lithium hexafluorophosphate ($LiPF_6$) and lithium bis(trifluoromethylsulfonyl)imide (LiTFSI) was kindly provided by Morita Chemical Industries Co., Ltd. and used as received. All the other chemicals used in this work were of A.R. grade.

2.2. Synthesis of the IL, 1g13TFSI and monomers, guanidinium bromides

The IL of 1g13TFSI and monomers of guanidinium bromides were synthesized by our reported papers [24,25]. The produced guanidinium bromides and lithium bis(trifluoromethylsulfonyl)imide (LiTFSI) were dissolved in deionized water and mixed for 24 h at ambient temperature. The crude ILs were dissolved with dichloromethane, and washed with deionized water until no residual halide anions, which were detected with the saturated solution of $AgNO_3$. The dichloromethane was removed by rotating evaporation. The product was dried under high vacuum for more than 24 h at 100 °C. The structure of synthesized monomers, guanidinium bromides (1g3), was confirmed by ^{1}H NMR and ^{13}C NMR.

1g3, ^{1}H NMR (400 MHz, $CDCl_3$), δ (TMS, ppm): 5.69 (NCH_2CHCH_2), 5.32 (NCH_2CHCH_2), 3.72 (NCH_2CHCH$_2$), 2.93 (m, 12H), 1.64 (NCH_2CH_2CH$_3$), 1.43 (NCH_2CH_2CH$_3$), 0.87 (NCH_2CH$_2$CH_3). ^{13}C NMR: (400 M Hz, $CDCl_3$), δ (TMS, ppm): 163.4, 131.5, 121.1, 52.7, 51.5, 40.1, 20.8, 10.9.

2.3. Polymerization of the IL monomers and preparation of PILs with TFSI$^-$ anions

The PILs were synthesized by a bulk polymerization method. The guanidinium bromide, methyl acrylate, acetonitrile and AIBN, at a ratio of 1.0 mol% to the amount of methacryl groups present in the solution, were mixed until they became homogeneous. The mixture was degassed in vacuum at 50 °C, and kept standing at 70 °C for 40 h. After polymerization, the obtained polymer, denoted as 1g3-MA-Br, was dried under vacuum at 60 °C for 24 h and 80 °C for 6 h. And
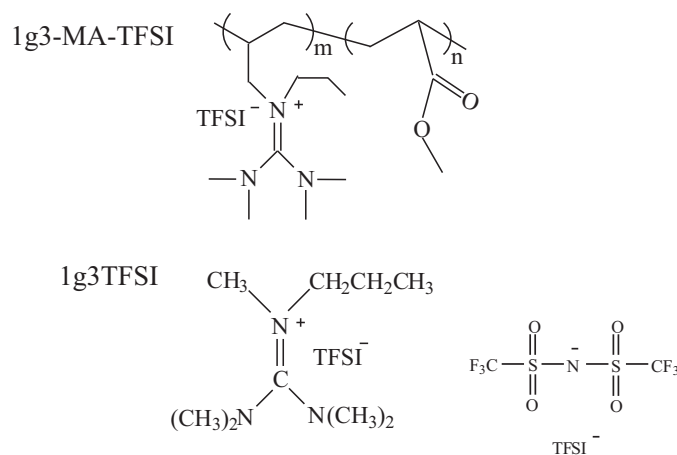
Scheme 1. The main components of the quaternary polymer electrolytes: the chemical structure of PIL, 1g3-MA-TFSI and IL, 1g3TFSI.

the structure of 1g3-MA-Br (depicted in Scheme 1) was confirmed by ^{1}H NMR and FT-IR.

1g3-MA-Br, ^{1}H NMR, (400 MHz, $CDCl_3$), δ (TMS, ppm): 3.65 (CHCOOCH_3), 3.14 (NCH_2CH), 3.10 (NCH_2CH$_2$CH$_3$), 2.88 [CN(CH_3)$_2$]$_2$, 2.35 (CHCOOCH$_3$), 1.89 (NCH_2CH), 1.72 (CH_2CHCOO), 1.56 (NCH_2CH_2CH$_3$) 1.29 (NCH_2CHCH_2), 0.90 (NCH_2CH$_2$CH_3).

1g3-MA-Br, FT-IR (KBr), ν (cm^{-1}): 3450 (H_2O), 2923, 2859, 2819 (CH_3, CH_2, CH), 1725 (C=O), 1606 (C=N), 1547 (C–N), 1158 (C–O).

To prepare PILs with TFSI$^-$ anions by a simple ion-exchange method, 1.2 g of 1g3-MA-Br was dissolved in 5 mL acetone, stirred for 2 h and then lithium salt (LiTFSI) at a molar ratio of 1.2 to the feed of guanidinium cations present in 1g3-MA-Br was added into the solution, and then stirred for another 4 h. After the ion-exchange reaction finished, the solution was poured into Teflon dishes and air-dried at 80 °C for 4 h. Then the obtained PILs were immersed in deionized water at 40 °C for 1 h, and rinsed with large amounts of deionized water. The process of immersion and rinse was repeated twice so as to remove the superfluous lithium salts. After that, the polymer was dried in vacuum at 80 °C for 24 h and the pure 1g3-MA-TFSI were obtained, whose chemical structure was confirmed by FT-IR.

FT-IR (KBr), 1g3-MA-TFSI, ν (cm^{-1}): 2992, 2956, 2846 (CH_3, CH_2, CH), 1735 (C=O), 1605 (C=N), 1560 (C–N), 1169 (C–O), (TFSI$^-$): 1349, 1199, 1159, 1064, 848 and 558.

M_n = 23570, M_w/M_n = 2.86, (GPC, polystyrene). Anal. Calcd. for 1g3-MA-TFSI: C 48.6, N 1.56. Found: C 48.7; N 1.57.

2.4. Preparation of the quaternary polymer electrolytes

The quaternary polymer electrolytes were prepared by separately dissolving the 1g3-MA-TFSI, 1g13TFSI, LiTFSI and nano-scale SiO_2 in acetone at 40 °C for 5 h and, then, mixed in three different proportions (Table 1). The solution was casted onto PTFE slides to prepare the electrolyte films. Then the film was dried in the air at room temperature for 12 h and subsequently dried at 80 °C under vacuum for another 12 h.

Table 1
Composition of PIL–LiTFSI–1g13TFSI–SiO$_2$ quaternary polymer electrolytes.

Sample name	Weight (g)				1g13TFSI/PIL ratio
	PIL	LiTFSI	Nano-scale SiO$_2$	1g13TFSI	wt/wt
Sample A	0.6	0.12	0.06	0.3	0.5
Sample B	0.6	0.12	0.06	0.27	0.45
Sample C	0.6	0.12	0.06	0.24	0.4

2.5. Preparation of batteries

Lithium foil (battery grade) was used as a negative electrode. And positive electrode was fabricated by spreading the mixture of LiFePO$_4$, acetylene black and PVdF (initially dissolved in N-methyl-2-pyrrolidone) with a weight ratio of 8:1:1 onto Al current collector (battery use). Loading of active material was about 2.5 mg cm^{-2} corresponding to 0.4 mAh cm^{-2} and this thinner electrode was directly used without pressing. Li/LiFePO$_4$ polymer batteries were fabricated (in dry-room) by laminating the lithium foil, a PIL–LiTFSI–1g13TFSI–SiO$_2$ quaternary polymer electrolyte membrane and a LiFePO$_4$ cathode tape.

2.6. Characterization methods

Structures of the synthesized ionic liquid monomer and the PILs were confirmed by ^{1}H NMR and ^{13}C NMR spectroscopy (Avance III 400) and tetramethylsilane was used as the internal reference for the analysis. The FT IR spectroscopic measurements were performed on a Bruker IFS-28 FT-IR spectrometer. Thermal analyses of the polymers were performed on a Perkin-Elmer TGA (Thermogravimetric analysis) from room temperature to 500 °C under nitrogen at a heating rate of 20 °C min^{-1}. Molecular weights of the polymers were estimated by Waters associates gel permeation chromatography (GPC) using 12 monodisperse polystyrenes (molecular weight range 10^2–10^7) as calibration standards. Elemental composition (C and N) was determined by an elemental analyzer (Perkin–Elmer 2400 II).

The ionic conductivity of the PILs was measured by the complex impedance method using a CHI660B Electrochemical Workstation. The electrolytes were placed between a pair of blocking electrodes. The data were collected over a frequency range 0.1–10^5 Hz with the amplitude of 5 mV for an open circuit potential. The ionic conductivity (σ) was calculated from the bulk electrolyte resistance value (R) found in the complex impedance diagram according to the following equation:

$$\sigma = \frac{L}{R \cdot S}$$

where L is the thickness of the polymer electrolyte film and S is the area of the polymer electrolyte film.

The electrochemical stability of the PILs electrolytes was determined on the CHI660B Electrochemical Workstation by linear sweep voltammetry (LSV) using the cell Li/PILs electrolyte/SS, in which the SS was used as working electrode, the lithium as the reference and the counter electrodes. The scanning rate is 1 mV s^{-1}.

Preliminary cycling tests on Li/LiFePO$_4$ polymer batteries were performed at 80 °C using a CT2001A cell test instrument (LAND Electronic Co., Ltd.). The discharge current rates were ranged from C/10 (0.04) to 1C (0.4 mA cm^{-2}) while the charge rate was fixed to C/10. The voltage cut-offs were fixed at 4.0 V (charge step) and 2.0 V (discharge step), respectively.

3. Results and discussion

3.1. Characterization of the PILs, 1g3-MA-TFSI

Fig. 1 shows the ^{1}H NMR spectra of the monomer 1g3 and the PILs 1g3-MA-TFSI. For 1g3, the assignments of corresponding protons are shown in Fig. 1(a). The characteristic proton absorptions in double bonds locate at δ 5.69 (CH$_2$CHCH$_2$) and 5.32 ppm (CH$_2$CHCH_2) in the structure of 1g3, and the absorptions completely disappear after polymerization as shown in Fig. 1(b), which indicates the polymerization carries out entirely and the product is relatively pure. The proton absorptions of δ 3.72 (NCH_2CHCH$_2$) and 2.93 ppm [CN(CH_3)$_2$] in Fig. 1(a) resulting from the character-
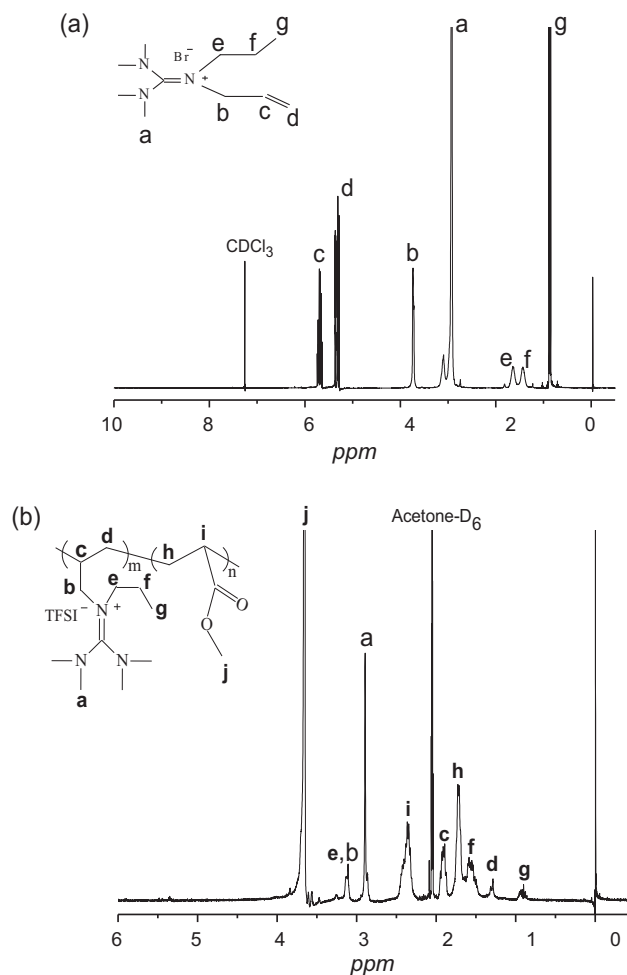

Fig. 1. ^{1}H NMR spectra of (a) the monomer, 1g3 and (b) the PIL, 1g3-MA-TFSI.

istic absorptions of guanidinium group still exist in the spectra of 1g3-MA-TFSI after the polymerization. Additionally, in Fig. 1(b), the peak at 3.65 (COOCH_3) results from methacrylate and the other assignments of protons are also marked.

Fig. 2 presents the FT IR spectra of 1g3-MA-TFSI having TFSI$^-$ counter-anion. In Fig. 2 the polymer show characteristic bands at 1735 and 1169 cm^{-1} for the C=O and C–O stretching vibration from
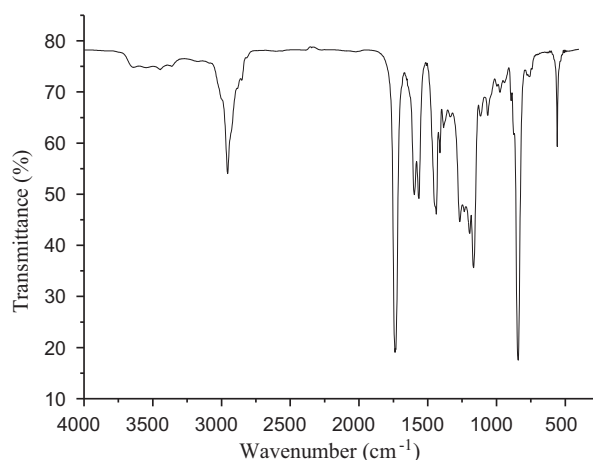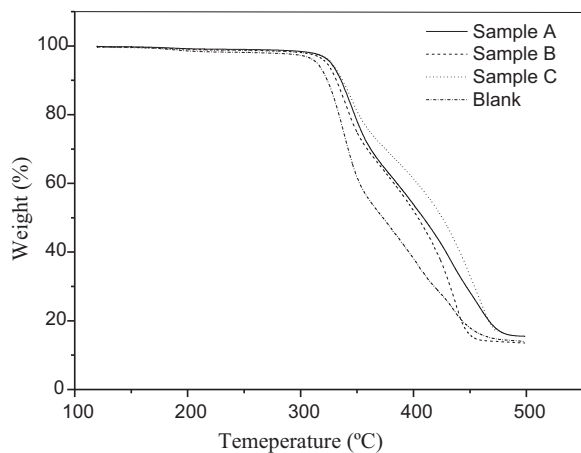

Fig. 2. IR spectra of 1g3-MA-TFSI.

Fig. 3. TGA profiles of pure PIL, 1g3-MA-TFSI and PIL–1g13TFSI–LiTFSI–SiO$_2$ polymer electrolytes with different 1g13TFSI amounts.

Fig. 4. DSC profiles of pure 1g3-MA-TFSI and PIL–1g13TFSI–LiTFSI–SiO$_2$ electrolyte samples with different 1g13TFSI contents.

the ester group, respectively. The neighbored bands centered near 1605 cm^{-1} and 1560 cm^{-1} most likely arise from the C=N and C–N stretching from the guanidinium cations. In addition, the characteristic bands [20,26,27] of the TFSI^{-} anion, such as 1349, 1199, 1159, 1064, 848 and 558 cm^{-1}, have been also observed in the figure. Combining the assignments of ^{1}H NMR and FT IR spectra, it indicated that 1g3-MA-TFSI had the expected chemical structure and moreover its purity was desirable.

For the 1g3-MA-TFSI used in lithium batteries, a quaternary polymer electrolyte based on 1g3-MA-TFSI as polymer host in combination with a guanidinium ionic liquid (1g13TFSI), LiTFSI salt and nano-size SiO$_2$ was prepared. The addition of ILs into the polymer electrolyte can improve the interfacial property toward the electrode material and increase the lithium ionic conductivity [16,19]. 1g13TFSI is used here because of its good electrochemical properties and exceptional battery performance as electrolytes. Nano-size SiO$_2$ is also added in this gel polymer electrolyte because it can enhance the mechanical strength and Lithium ion transference number [6].

3.2. Thermal properties of the PIL and PIL-based polymer electrolyte

The thermal stability of the pure PIL and PIL-based electrolytes was characterized by TGA, as shown in Fig. 3. It was obvious that both the pure PIL and PIL–1g13TFSI–LiTFSI–SiO$_2$ electrolyte samples showed similar thermal decomposition behaviors and they all decomposed in two steps. The decomposition temperature of the electrolyte samples were not obviously affected by the contents of 1g13TFSI, whose decomposition temperature was 415.4 °C [28]. Furthermore, the PIL-based electrolyte samples were found to be thermal stable up to 320 °C.

Fig. 4 shows the DSC profiles of the pure 1g3-MA-TFSI and the PIL–1g13TFSI–LiTFSI–SiO$_2$ electrolyte samples at different 1g13TFSI amounts. The pure 1g3-MA-TFSI presented a glass transition feature (T_g) around 15 °C. The amount of 1g13TFSI distinctly affected the glass phase transition. With the increase of 1g13TFSI, T_g of the PILs-based electrolyte samples decreased drastically. When the amount of 1g13TFSI reached 45 wt%, T_g of the electrolyte samples dropped below −60 °C. This decrease in T_g may be attributed to 1g13TFSI served as a plasticizer in the electrolyte samples, which promotes the distancing of the PIL chains and changes the crystalline structure leading to a considerable increase of amorphous phase, as already observed by Pawlicka et al. [29]. At higher IL amounts, it did not appear any endothermic peaks in the DCS
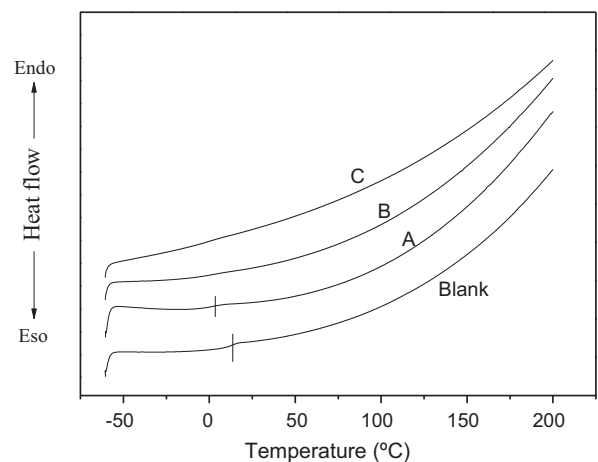
profiles. This result was different when compared with the result of pyrrolidinium-based PIL electrolytes containing pyrrolidinium-based ILs and reported by Appetecchi et al. [19], who found a small endothermic peak at higher IL amounts. They suggested that it was a lithium salt/ionic liquid phase separation within the PIL-based electrolytes above an IL content equal to 44 wt%.

3.3. Electrochemical stability and ionic conductivity

Electrochemical stabilities of the PIL-based electrolyte samples at 80 °C were characterized by linear sweep voltammetry, as shown in Fig. 5. The IL content did not affect the electrochemical stability of the PIL-based electrolytes. They decomposed at about 4.0 V vs. Li/Li$^+$, which was suitable for the application in Li/LiFePO$_4$ battery as a polymer electrolyte at 80 °C.

Fig. 6 shows the temperature dependence of the ionic conductivity of PIL–1g13TFSI–LiTFSI–SiO$_2$ electrolyte samples. For the samples, a linear increase was observed in the conductivity values with temperature, which fitted an Arrehenius-type behavior, typically obtained in completely amorphous phase ionic conductivity [29]. Additionally, it was also obvious from Fig. 4 that the ionic conductivity enhanced markedly with increasing the IL content, which was attributed to the increase of amorphous content by the plasticization of 1g13TFSI. This phenomenon was in good
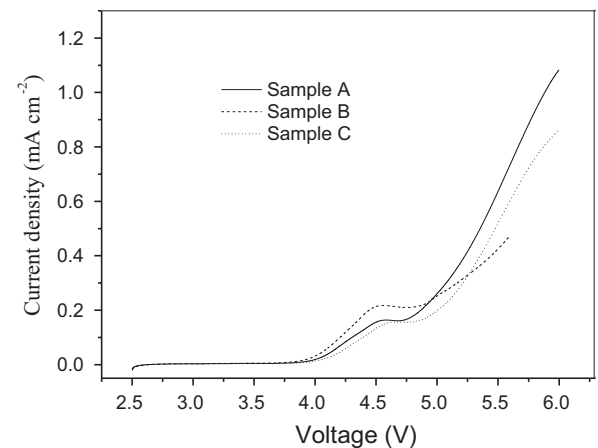

Fig. 5. Electrochemical stability of PIL–1g13TFSI–LiTFSI–SiO$_2$ electrolyte samples with different 1g13TFSI contents at 80 °C. (Li/PIL electrolyte/SS cell, 10 mV s^{-1}, 2.5~6.0 V.)
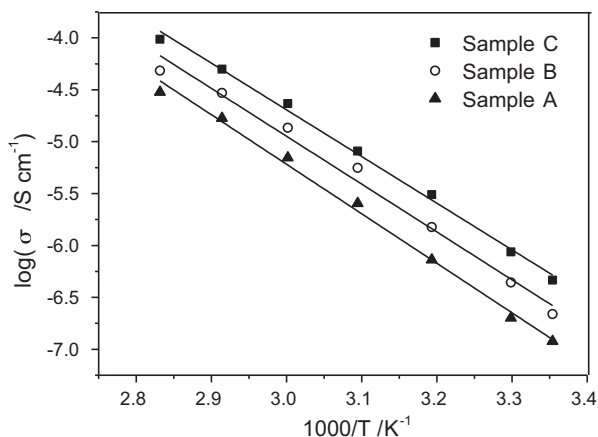
Fig. 6. Temperature dependence of the ionic conductivity of PIL–1g13TFSI–LiTFSI–SiO$_2$ electrolyte samples with different 1g13TFSI contents.

agreement with the thermal measurements of Fig. 2. The sample C presented a higher ionic conductivity at 80 °C, and it was 1.17×10^{-4} S cm^{-1}.

3.4. Lithium redox in the PIL-based polymer electrolyte

Lithium redox in the PIL-based polymer electrolyte was characterized by cyclic voltammograms (CVs), as seen in Fig. 7. The plating of lithium on the nickel electrode can be clearly observed like 1g13TFSI IL electrolytes [24]. In the first cycle for the PIL-based polymer electrolyte, the cathodic peak corresponding to the plating of lithium was about −0.18 V vs. Li/Li$^+$, and in the returning scan the anodic peak corresponding to the stripping of lithium was around 0.19 V vs. Li/Li$^+$. The lithium redox in the PIL-based polymer electrolyte might be caused by the generation of a certain surface film (SEI) on the Ni electrode. The cathodic peak currents decreased gradually with the cycle number. This suggested that the SEI film turned thicker so that the lithium reduction was restrained markedly. The broad cathodic peak, ranging from 0.95 V to −0.16 V vs. Li/Li$^+$, might be assigned to the electrochemical reduction of the electrolyte, and at the same time it could be presumed that this reduction might generate the SEI film on Ni electrode. Furthermore, the extension of this peak significantly decreased in the following scans, so it could mean that SEI film generating in the first cycle also restrained the reduction of the electrolyte. Additionally, one cathodic peak in the range from 1.8 V to 1.0 V vs. Li/Li$^+$ was found in the first cycle, which might be caused by the reactions of the trace water or oxygen in the PIL-based electrolyte on the Ni elec-
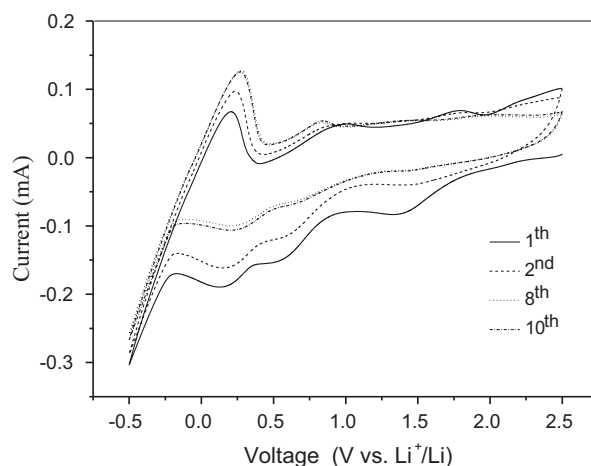

Fig. 7. Cyclic voltammograms for PIL–1g13TFSI–LiTFSI–SiO$_2$ electrolyte (sample C). Working electrode: Ni; counter electrode and reference electrode: lithium; scan rate: 10 mV s^{-1}.

trode [30], and this peak disappeared in the third and eighth cycles due to the SEI film forming.

3.5. Interfacial property with lithium electrode

The interfacial property between anode and electrolyte in a lithium secondary battery is one of important factors that determined the safety and cyclic stability of the battery [31]. Interfacial stability of the PIL-based polymer electrolyte with the lithium metal electrode was estimated by electrochemical impedance spectroscopy. Fig. 8 shows the time evolution of the impedance spectra of a symmetrical Li/PIL–1g13TFSI–LiTFSI–SiO$_2$/Li cell at 80 °C under open-circuit conditions. The intercept with real axis of the spectra at high frequency was assigned to the electrolyte bulk resistance (R_b), and the diameter of the semicircle was assigned to the interfacial resistance (R_i) of the quaternary polymer electrolyte/lithium metal. For the PIL-based polymer electrolyte, its R_b was almost unchangeable during 6 days. But a marked increase of R_i was observed during the initial period of storage and then it started to decrease after 2 days. In the following test R_i was found to be constant, leveling at 1800 Ω after 5 days storage. This behavior, commonly also observed in other IL-based polymer electrolytes [13,16], is due to the reaction between the lithium electrode and the polymer electrolyte forming a passivation layer (SEI) onto the lithium anode that protects the electrode from further reaction. Furthermore, the passivation layer restricted the reaction between the electrolyte and lithium metal gradually,
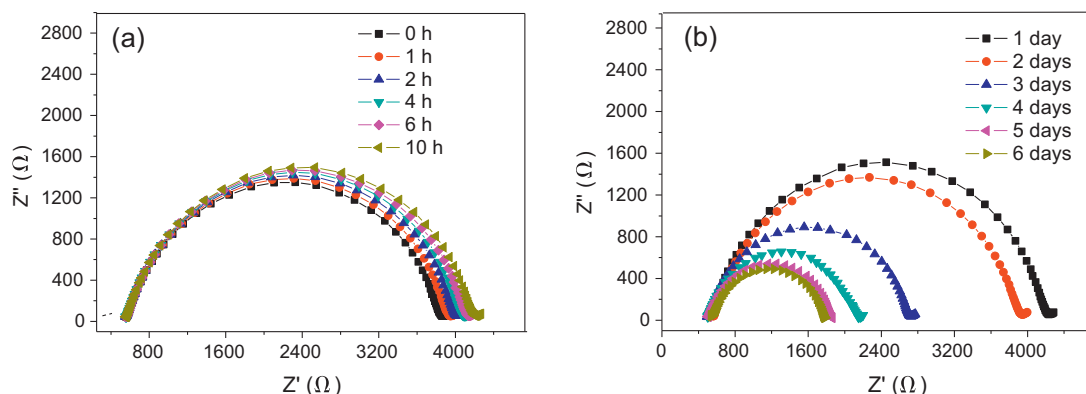

Fig. 8. Time evolution of the impedance spectra of symmetrical Li/(PIL–1g13TFSI–LiTFSI–SiO$_2$)/Li cells: (a) from 0 to 10 h, (b) from 1 to 6 days at 80 °C.
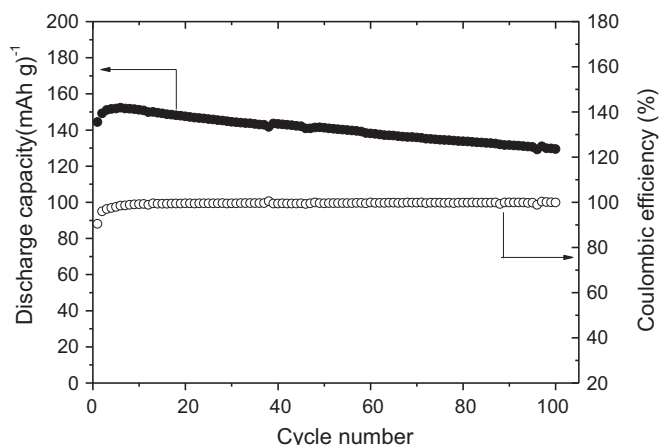
Fig. 9. Discharge capacity and coulombic efficiency as functions of cycle number for Li/(PIL–1g13TFSI–LiTFSI–SiO$_2$)/LiFePO$_4$ cells at 80 °C. Charge–discharge current rate is 0.1 C.
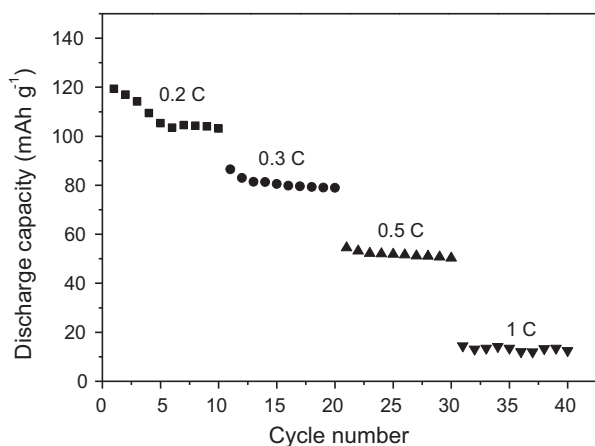

Fig. 10. Specific capacities against cycle number for Li/(PIL–1g13TFSI–LiTFSI–SiO$_2$)/LiFePO$_4$ cells at different charge/discharge rates at 80 °C. Charge current rate is fixed at 0.1C.

and a dynamic equilibrium could be achieved after some time. This issue is in good agreement with the CVs measurements of Fig. 7.

3.6. Charge-discharge performance of batteries

The charge–discharge (C–D) performance of Li/PIL-based polymer electrolytes/LiFePO$_4$ batteries had been characterized at 80 °C, and their cycling properties were presented in Fig. 9. The discharge capacity and the coulombic efficiency of the battery were found to be 144 mAh g^{-1} and 90% in the first cycle, respectively. During the initial 5 cycles, the discharge capacity and the culombic efficiency increased gradually, perhaps as a result of generation of improved penetration and contact of the IL component from the electrolyte into the electrode material [32]. After an increasing step, the cell delivered a maximum capacity of about 156 mAh g^{-1} (corresponding to 92% of theoretical capacity) at 0.1C. The cell was cycled for 100 cycles with a capacity fading of approximately 0.17 mAh g^{-1} percycle. After 100 cycles, the discharge capacity of the battery was still higher and it retained 140 mAh g^{-1}.

Additionally, the performance of Li/PIL-based polymer electrolyte/LiFePO$_4$ cell at different current rates was also determined, as seen in Fig. 10. Discharge capacity of the cell was found to decrease obviously as the discharge rates increased. The fall of discharge capacity at elevated current rates is associated with

low lithium ion transference number of the polymer electrolyte [15]. Next, we will take some measures to improve lithium ion transference number of the PIL-based polymer electrolyte. For example, the amounts of ionic liquid groups in polymer chains are increased by polymerization, which is favorable for dissociating lithium salts. As a result, lithium ion transference number and ionic conductivity will be improved, and, consequently, high discharge capacity of batteries might be obtained at higher current rates.

4. Conclusions

The electrochemical properties of solvent-free, quaternary polymer electrolytes based on a novel polymeric ionic liquid (PIL), 1g3-MA-TFSI as polymer host and incorporating 1g13TFSI ionic liquid and LiTFSI salt are reported. The properties of PILs containing different amount of 1g13TFSI ionic liquid were characterized. The PILs have good thermal stability and electrochemical stability, and they both start to decompose over 300 °C and 4.0 V. Particularly, the quaternary polymer electrolytes exhibit high lithium ion conductivity at high temperature, wide electrochemical stability window, time-stable interfacial resistance values and good lithium stripping/plating performance. The batteries assembled with the quaternary polymer electrolyte have good cycling stability at 80 °C, and they are capable to deliver 140 mAh g^{-1} at 0.1C rates with very good capacity retention.

References

[1] J.M. Tarascon, M. Armand, Nature 414 (2001) 359.
[2] F. Croce, G.B. Appetecchi, L. Persi, B. Scrosati, Nature 394 (1998) 456.
[3] K.M. Abraham, Z. Jiang, B. Carroll, Chem. Mater. 9 (1997) 1978.
[4] M.C. Borghini, M. Mastragostino, S. Passerini, B. Scrosati, J. Electrochem. Soc. 142 (1995) 2118.
[5] J.-H. Shin, W.A. Henderson, S. Scaccia, P.P. Prosini, S. Passerini, J. Power Sources 156 (2006) 560.
[6] S. Ferrari, E. Quartarone, P. Mustarelli, A. Magistris, M. Fagnoni, S. Protti, C. Gerbaldi, A. Spinella, J. Power Sources 195 (2010) 559.
[7] D.W. Kim, S.R. Sivakkumar, D.R. MacFarlane, M. Forsyth, Y.K. Sun, J. Power Sources 180 (2008) 591.
[8] J.H. Shin, W.A. Henderson, C. Tizzani, S. Passerini, S.S. Jeong, K.W. Kim, J. Electrochem. Soc. 153 (2006).
[9] P. Raghavan, X. Zhao, C. Shin, D.H. Baek, J.W. Choi, J. Manuel, M.Y. Heo, J.H. Ahn, C. Nah, J. Power Sources 195 (2010) 6088.
[10] J.H. Shin, W.A. Henderson, S. Scaccia, P.P. Prosini, S. Passerini, J. Power Sources 156 (2006) 560.
[11] G.T. Kim, G.B. Appetecchi, F. Alessandrini, S. Passerini, J. Power Sources 171 (2007) 861.
[12] K.-S. Liao, T.E. Sutto, E. Andreoli, P. Ajayan, K.A. McGrady, S.A. Curran, J. Power Sources 195 (2010) 867.
[13] P. Raghavan, X. Zhao, J. Manuel, G.S. Chauhan, J.-H. Ahn, H.-S. Ryu, H.-J. Ahn, K.-W. Kim, C. Nah, Electrochim. Acta 55 (2010) 1347.
[14] S.R. Sivakkumar, D.R. MacFarlane, M. Forsyth, D.W. Kim, J. Electrochem. Soc. 154 (2007) A834.
[15] H. Ye, J. Huang, J.J. Xu, A. Khalfan, S.G. Greenbaum, J. Electrochem. Soc. 154 (2007).
[16] C. Sirisopanaporn, A. Fernicola, B. Scrosati, J. Power Sources 186 (2009) 490.
[17] S.Y. Chew, J. Sun, J. Wang, H. Liu, M. Forsyth, D.R. MacFarlane, Electrochim. Acta 53 (2008) 6460.
[18] O. Green, S. Grubjesic, S. Lee, M.A. Firestone, Polym. Rev. 49 (2009) 339.
[19] G.B. Appetecchi, G.T. Kim, M. Montanino, M. Carewska, R. Marcilla, D. Mecerreyes, I. De Meatza, J. Power Sources 195 (2010) 3668.
[20] A.L. Pont, R. Marcilla, I. De Meatza, H. Grande, D. Mecerreyes, J. Power Sources 188 (2009) 558.
[21] M. Li, L. Yang, S. Fang, S. Dong, J. Membr. Sci. 366 (2011) 245.

[22] W. Ogihara, S. Washiro, H. Nakajima, H. Ohno, Electrochim. Acta 51 (2006) 2614.
[23] H. Ohno, M. Yoshizawa, W. Ogihara, Electrochim. Acta 50 (2004) 255.
[24] S.H. Fang, L. Yang, J.X. Wang, H.Q. Zhang, K. Tachibana, K. Kamijima, J. Power Sources 191 (2009) 619.
[25] S.H. Fang, L. Yang, J.X. Wang, M.T. Li, K. Tachibana, K. Kamijima, Electrochim. Acta 54 (2009) 4269.
[26] S. Rajendran, M.R. Prabhu, M.U. Rani, J. Power Sources 180 (2008) 880.
[27] Y. Umebayashi, T. Mitsugi, S. Fukuda, T. Fujimori, K. Fujii, R. Kanzaki, M. Takeuchi, S.I. Ishiguro, J. Phys. Chem. B 111 (2007) 13028.
[28] S.H. Fang, L. Yang, C. Wei, C. Jiang, K. Tachibana, K. Kamijima, Electrochim. Acta 54 (2009) 1752.
[29] A. Pawlicka, M. Danczuk, W. Wieczorek, E. Zygadło-Monikowska, J. Phys. Chem. A 112 (2008) 8888.
[30] S. Fang, Z. Zhang, Y. Jin, L. Yang, S.-i. Hirano, K. Tachibana, S. Katayama, J Power Sources 196 (2011) 5637.
[31] Y.G. Lee, J.K. Park, S.I. Moon, Electrochim. Acta 46 (2000) 533.
[32] J.H. Shin, W.A. Henderson, S. Passerini, J. Electrochem. Soc. 152 (2005) A978.